GEOPHYSICAL RESEARCH LETTERS, VOL. 37, L13605, doi:10.1029/2010GL043623, 2010



# Ocean tomography with acoustic daylight

Oleg A. Godin,[1,2] Nikolay A. Zabotin,[1,3] and Valery V. Goncharov[4]

Received 14 April 2010; revised 3 June 2010; accepted 8 June 2010; published 9 July 2010.

[1] Ambient noise in the ocean provides acoustic illumination, which can be used, similarly to daylight in the atmosphere, to visualize objects and characterize the environment. It has been shown theoretically that deterministic travel times between any two points in a moving or motionless, inhomogeneous, time-independent medium can be retrieved from the cross-correlation function of diffuse acoustic noise recorded at the two points, without a detailed knowledge of the noise field's sources or properties. In this paper, techniques are developed to account for receiver motion and suppress contributions due to powerful transient localized noise sources, such as nearby shipping, in order to enhance noise diffusivity. The data-processing techniques are applied to ambient noise recordings of opportunity, which were obtained as a by-product of a long-range sound propagation experiment in the Pacific Ocean. The feasibility of passive ocean acoustic tomography with ambient noise recorded at two vertical line arrays is demonstrated successfully. **Citation:** Godin, O. A., N. A. Zabotin, and V. V. Goncharov (2010), Ocean tomography with acoustic daylight, *Geophys. Res. Lett.*, *37*, L13605, doi:10.1029/2010GL043623.

## 1. Introduction

[2] Acoustic illumination due to underwater diffuse noise, akin to daylight in the atmosphere, can be used as means to visualize objects and characterize the environment. In an inhomogeneous fluid, sound speed and fluid velocity fields can be retrieved from cross-correlations of noise measured at a sufficient number of points [*Rickett and Claerbout*, 1999; *Godin*, 2006]. Compared to well-established seismic interferometry [*Wapenaar et al.*, 2008], passive ocean acoustic tomography faces a number of unique challenges, including time-dependence of the environment, motion of receivers and the medium, and requirements of very high relative accuracy of measurements of the sound speed in water. While coherent wavefronts have been identified in noise cross-correlations [*Roux et al.*, 2004; *Fried et al.*, 2008; *Brooks and Gerstoft*, 2009], and noise interferometry is successfully used to study the ocean bottom [*Siderius et al.*, 2010], no applications of the technique to quantitative characterization of the water column have been reported to date.

[3] This paper presents the first experimental demonstration of passive acoustic tomography in the ocean and demonstrates the feasibility of sound-speed measurements with oceanographically relevant accuracy. Because of its low capital costs, the ability to provide long time series of data, and a negligible impact on the environment, including marine mammals, acoustic tomography with ambient noise may find applications in various ocean observing systems, where the traditional tomography, which relies on powerful man-made sound sources, is deemed too expensive or too invasive.

## 2. NPAL Billboard Array Experiment

[4] The Billboard Array experiment was carried out in 1998–1999 as part of the North Pacific Acoustic Laboratory (NPAL) program designed to investigate low-frequency, long-range sound propagation in the ocean [*Worcester and Spindel*, 2005]. Five vertical line arrays (VLAs) of hydrophones were installed on subsurface moorings in 1800-m-deep water on the continental shelf off Point Sur, California (see auxiliary material).[5] Nominal depths (in meters) of hydrophones on VLAs 1 to 4 and VLA5 are 400 + 37.5 ($n$ − 1) and 200 + 37.5 ($n$ − 1), respectively, where $n$ is the hydrophone number ($n$ = 1…20 for VLAs 1 to 4, $n$ = 1…40 for VLA 5). The horizontal separation of VLA pairs ranged from about 500 m between VLAs 1 and 2 to about 3500 m between VLAs 1 and 5. Acoustic pressure was recorded in segments of 20 min duration every four hours in a wide frequency band from about 6 to 130 Hz at 300 Hz sampling rate. The motion of array elements was monitored with a network of transponders located on the ocean bottom. The positions of hydrophones in the VLAs were known within a few cm.

[5] The Billboard Array site was close to shipping lanes, the known migration routes of marine mammals, and epicenters of micro-earthquakes associated with convergence of the North American and Pacific Ocean plates [*Worcester and Spindel*, 2005; *Baggeroer et al.*, 2005]. In individual data segments, localized, transient noise sources either of biological origin or due to nearby shipping and micro-earthquakes usually dominate over contributions of distributed noise sources, such as distant shipping and breaking water waves on the ocean surface. Many data records also included rather weak phase-manipulated coherent signals radiated by an acoustic source thousands of kilometers away from the array. In what follows, acoustic pressure recorded by the Billboard Array will be referred to as ambient noise

[1]Cooperative Institute for Research in Environmental Sciences, University of Colorado at Boulder, Boulder, Colorado, USA.
[2]Earth System Research Laboratory, NOAA, Boulder, Colorado, USA.
[3]Department of Electrical and Computer Engineering, University of Colorado at Boulder, Boulder, Colorado, USA.
[4]P. P. Shirshov Oceanology Institute, Russian Academy of Sciences, Moscow, Russia.


0094-8276/10/2010GL043623

[5]Auxiliary materials are available in the HTML. doi:10.1029/2010GL043623.

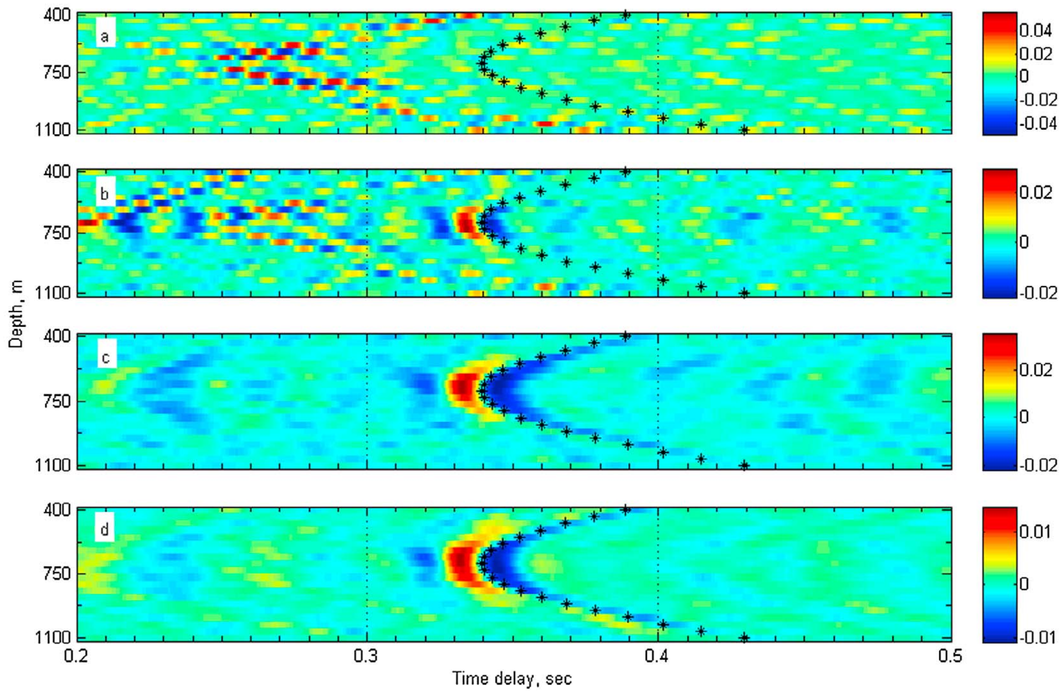


**Figure 1.** Estimates of ambient noise cross-correlation function obtained using various averaging times: (a) 20 min, (b) 1 hour, (c) 8 hours, and (d) 75 hours. The estimates shown in Figures 1a–1d are obtained by correlating the acoustic pressures recorded on hydrophone #9 of VLA 1 and all 20 hydrophones of VLA 2. Asterisks show the deterministic travel times between each pair of hydrophones. The travel times are calculated using a nominal sound-speed profile.

regardless of a particular sound generation mechanism prevalent in a specific data segment.

## 3. Noise Cross-Correlation Function

[6] Cross-correlation function $C(\mathbf{x}_1,\mathbf{x}_2,\tau)$ of time series of random diffuse noise $p(\mathbf{x},t)$ recorded at points $\mathbf{x}_1$ and $\mathbf{x}_2$ is theoretically predicted to reproduce wavefronts of the sum of two deterministic Green's functions (impulse responses of the medium): a field $G(\mathbf{x}_2,\mathbf{x}_1,\tau)$ radiated by a point source at $\mathbf{x}_1$ and received at $\mathbf{x}_2$ and $G(\mathbf{x}_1,\mathbf{x}_2,-\tau)$; that is, time reversal of the field propagating from $\mathbf{x}_2$ to $\mathbf{x}_1$ [*Rickett and Claerbout*, 1999; *Godin*, 2006; *Wapenaar et al.*, 2008]. For the wavefronts' reproduction, unlike reproduction of the exact Green's functions, the noise field is not required to be perfectly diffuse (i.e., isotropic and spatially uniform) [*Snieder*, 2004; *Godin*, 2006]; noise sources are not required to be delta-correlated or motionless [*Godin*, 2009a]. In the experiment, the noise cross-correlation function (NCCF) is estimated by averaging over time a product of signals recorded by two hydrophones:

$$C(\mathbf{x}_1,\mathbf{x}_2,\tau) = T^{-1}\int_{-T/2}^{T/2} dt\; p(\mathbf{x}_1,t+\tau)p(\mathbf{x}_2,t). \qquad (1)$$

For a particular ray connecting two points, the averaging time $T$ necessary for the deterministic wavefronts to emerge is proportional to the square of the ratio of the total acoustic energy reaching one point to the energy propagating to that point along the ray through the first Fresnel zone in the vicinity of the other point (N. A. Zabotin and O. A. Godin, Emergence of acoustic Green' s functions from time averages of ambient noise, submitted to *Acta Acustica united with Acustica*, 2009).

[7] Correlating records made by individual hydrophones on two VLAs allows one to estimate the dependence of the NCCF on the time delay $\tau$ and depths of the receivers at a fixed horizontal separation. Figure 1 illustrates the evolution of the NCCF estimates with increasing averaging time. The number of data segments used ranges from 1 (Figure 1a) to 235 (Figure 1d). To suppress the effect of strong nearby sound sources and enhance noise diffusivity, acoustic pressure $p$ in equation (1) was replaced by 1 when $p > 0$, and $-1$ when $p < 0$. (This version of the cross-correlation function estimate is sometimes referred to as bit correlation.) The data sampling rate in the experiment, while relatively low, was higher than twice the highest acoustic frequency recorded and, according to the Shannon sampling theorem, allowed for reconstruction of signals as continuous functions of time. Trigonometric interpolation of recorded signals was used to calculate the time-delay dependence of the NCCF at a grid ten times finer than the data sampling. Hydrophone positioning information was used to recalculate short-term cross-correlation estimates from actual to nominal positions of the receivers prior to averaging over time intervals $T$ that involved more than one data segment.

[8] As expected, at large averaging times the NCCF estimates have strong peaks and troughs in the vicinity of a deterministic wavefront (Figures 1c and 1d), which in this case corresponds to direct (as opposed to surface and/or bottom reflected) rays connecting receivers on VLA 1 and VLA 2. (In Figure 1, the deterministic wavefront is represented by travel times from one point on VLA 1 to each hydrophone on VLA 2, and visualizes the travel-time dependence on receiver depth at a fixed horizontal separa-

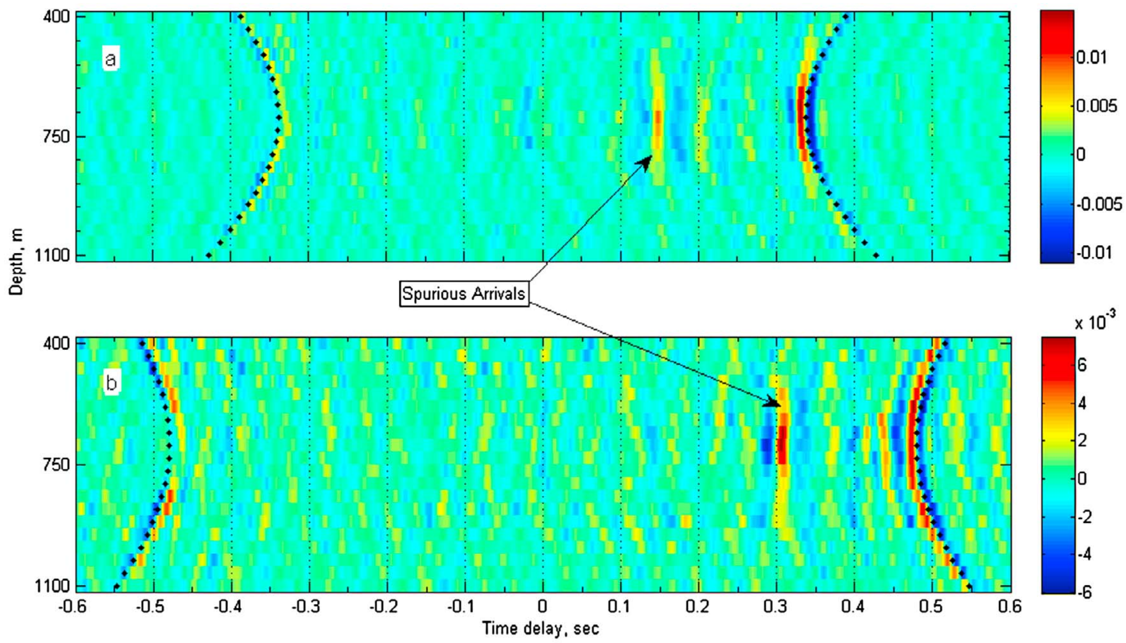


**Figure 2.** Long-term averages of the ambient noise. The NCCF estimates shown are obtained by correlating 100 hours of the acoustic pressures recorded on (a) hydrophone #9 of VLA 1 and all 20 hydrophones of VLA 2 and (b) on hydrophone #9 of VLA 3 and all 20 hydrophones of VLA 4. Asterisks show the deterministic travel times between each pair of hydrophones.

tion. In underwater acoustics, such a representation of a wavefront is referred to as "timefront.") In a single data segment (Figure 1a), a localized sound source dominates, and minima and maxima of the NCCF estimate lie away from the deterministic timefront. When a number of data segments are used, contributions of various localized, nearby sources are combined with contributions of distributed and distant noise sources, resulting in the NCCF peak and trough that bracket a deterministic timefront (Figures 1b and 1c). As the averaging time grows, the main peak and trough of the NCCF estimate increase in magnitude and extend along the deterministic timefront, while other peaks and troughs are washed out (Figures 1b and 1c). The averaging time needed for a reliable retrieval of a deterministic timefront from the NCCF was found to range from several hours at horizontal separations of ~0.5 km to ~40 hours at the largest horizontal separation of 3.5 km. These values are larger than theoretical estimates [*Gouédard et al.*, 2008; Zabotin and Godin, submitted manuscript, 2009] of ~10 min and ~8 hours, respectively, obtained assuming diffuse, isotropic noise. The difference is the result of a preponderance of localized noise sources at the experimental site.

[9] Long-term noise averages reveal additional details of the NCCF (Figure 2). Unlike short-term averages, distinct peaks and troughs of the NCCF that bracket deterministic timefronts appear at $\tau < 0$ as well as at $\tau > 0$. The magnitudes of the peaks and troughs at $\tau > 0$ are much larger than at $\tau < 0$, indicating that intensity of diffuse noise propagating from north-northwest (from VLA1 to VLA 2 and from VLA 3 to VLA 4) is considerably larger than in the opposite direction. For sound propagating from north-northwest, the intensity of the diffuse component of the noise decreases with increasing grazing angle, and the bulk of the diffuse acoustic energy propagates within ±15° from horizontal. In contrast, for sound propagating from south-southeast, the intensity of the diffuse noise component has a minimum at near-horizontal directions. The pronounced azimuthal anisotropy of low-frequency noise propagating within the underwater sound channel is consistent with the presence of distant shipping and/or strong sources of wind-generated dynamic noise in the North Pacific. Nonreciprocity of sound propagation due to ocean currents leads to asymmetry of the positions of the NCCF peaks and troughs at $\tau < 0$ and $\tau > 0$ [*Godin*, 2006]. With the Billboard Array data, the asymmetry could not be measured with accuracy sufficient enough to evaluate the velocity of the currents.

[10] In addition to the NCCF peaks and troughs in the vicinity of timefronts of direct ray arrivals, long-term averages reveal additional robust features at earlier, positive time delays. These features are marked "spurious arrivals" in Figure 2. In all cases, time delays corresponding to the spurious arrivals are smaller than deterministic travel times between points on the two VLAs. Persistent noise sources distributed along a curve (Zabotin and Godin, submitted manuscript, 2009), such as a shipping lane or surf, as well as a localized noise source onshore can be responsible for the observed features. Further research is necessary to unambiguously determine the physical origin of the early spurious arrivals and assess their possible use for characterization of the environment.

[11] *Baggeroer et al.* [2005] established that statistics of the noise field at the experimental site exhibit strong deviations from Gaussianity when the field is dominated by localized noise sources. Therefore, the contributions of localized noise sources can be suppressed, and diffusivity of the noise field can be effectively enhanced by excluding data segments with non-Gaussian noise from time averages.

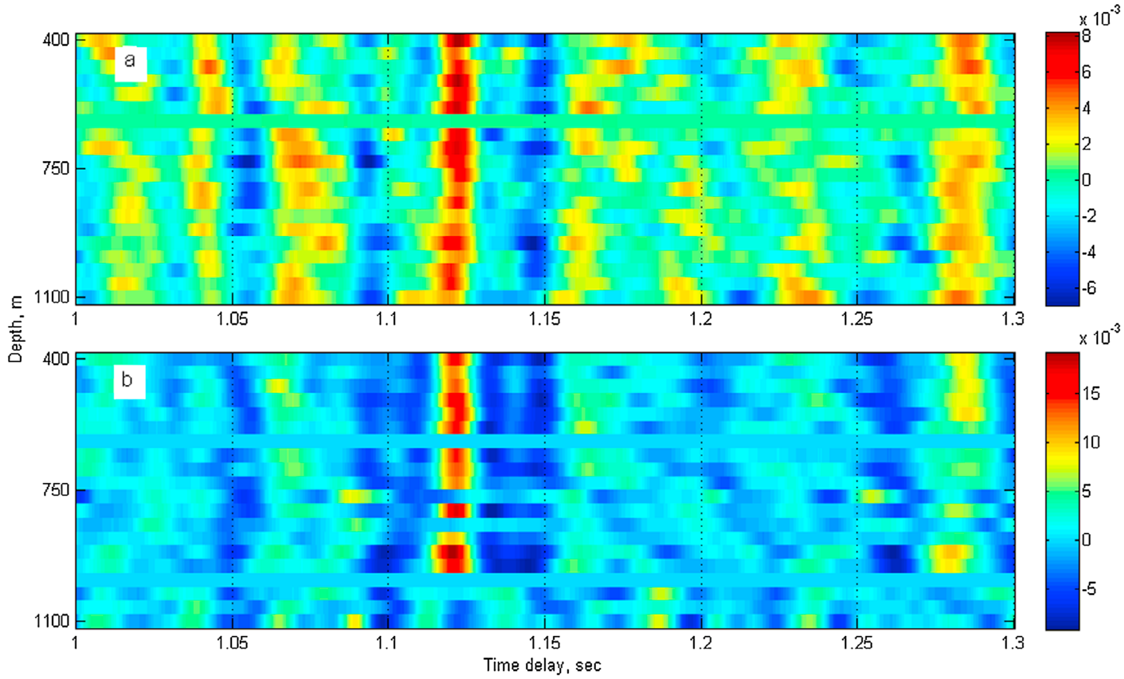


**Figure 3.** Suppression of transient sources of non-diffuse and non-Gaussian noise using "kurtosis screening" of the data. Estimates of the cross-correlation function of noise recorded on hydrophones located at the same nominal depth of VLAs 1 and 3 are obtained (a) without and (b) with "kurtosis screening." Noise records are averaged over 12 hours of observation.

This concept was implemented by requiring that excess kurtosis of a time series recorded by a hydrophone not exceed a certain threshold. As illustrated in Figure 3, the "kurtosis screening" technique typically eliminates or suppresses most peaks and troughs in the NCCF estimate except for the peaks and troughs in the vicinity of deterministic timefronts; helps to identify the NCCF features needed for environmental characterization; and improves the accuracy of the deterministic travel-time retrieval from the NCCF. The "kurtosis screening" ceases to be useful when most data segments exhibit non-Gaussian noise, and the number of remaining segments is insufficient for averaging. Furthermore, it was found that, in a number of cases, noise diffusivity also can be enhanced by averaging over a sufficiently large number of data segments, each of which is dominated by localized noise source(s).

## 4. Retrieval of the Sound Speed Profile

[12] Oceanographically-relevant sound-speed measurements with accuracy ~1 m/s require relative accuracy of acoustic travel time measurements of about 0.1%. It was shown theoretically that $C(\mathbf{x}_1,\mathbf{x}_2,\tau) = 0$ when the time delay $\tau$ equals the travel time along a ray that connects $\mathbf{x}_1$ and $\mathbf{x}_2$ without touching a caustic [*Godin*, 2009b, 2010]. This theoretical prediction is consistent with our experimental results, see Figures 1 and 2. Travel times along direct rays connecting hydrophones on various VLAs were found from the NCCF estimates as positions of those zero crossings that lie between the main peak and trough. With horizontal variation of the sound speed between VLAs being negligible, two techniques were used for retrieval of the vertical dependence of the sound speed $c$ from passively measured travel times. In a simple, blind inversion (Figure 4a), only travel times between hydrophones of the same number on two VLAs were used. The sound speed was calculated as the ratio of the distance between the hydrophones to the measured travel time, and assigned to the mid-depth of the hydrophones. No a priori environmental information is utilized in such an inversion. It can be shown that, because of relatively small horizontal separations of VLAs, neglect of the sound-speed variation along a ray leads to errors not exceeding 0.2 m/s. The inversion errors are dominated by errors in the travel-time measurement, which are caused by the difference between the NCCF and its estimate. The errors were evaluated for each hydrophone pair (Figure 4a) from the level of incoherent noise in the NCCF estimate relative to the contrast between the NCCF peak and trough.

[13] A more accurate and detailed reconstruction of the sound-speed profile is provided by a full tomographic inversion (Figure 4b). The inversion utilized up to $1 + 2N$, $N = 0, 1, \ldots, 5$ propagation paths for each hydrophone. The propagation paths for $N = 0$ are shown in Figure 4b by black dashed lines; additional propagation paths for $N = 3$ are illustrated for two hydrophones with red dashed lines. The travel-time inversion technique was originally developed [*Goncharov et al.*, 1997] for active ocean acoustic tomography. It assumes a linear relation between deviations of the sound-speed field and ray travel times from their values in a background environment. Regularization is used to solve the resulting overdetermined set of linear algebraic equations. The accuracy of the inversion is estimated from the travel-time measurement errors and the RMS mismatch between the measured travel times and their values in the reconstructed environment. In Figure 4b, the RMS sound speed-inversion errors range from 1.5 to 1.9 m/s, depending on $N$. The passively measured sound speed profiles presented in Figures 4a and 4b agree within their stated mea-

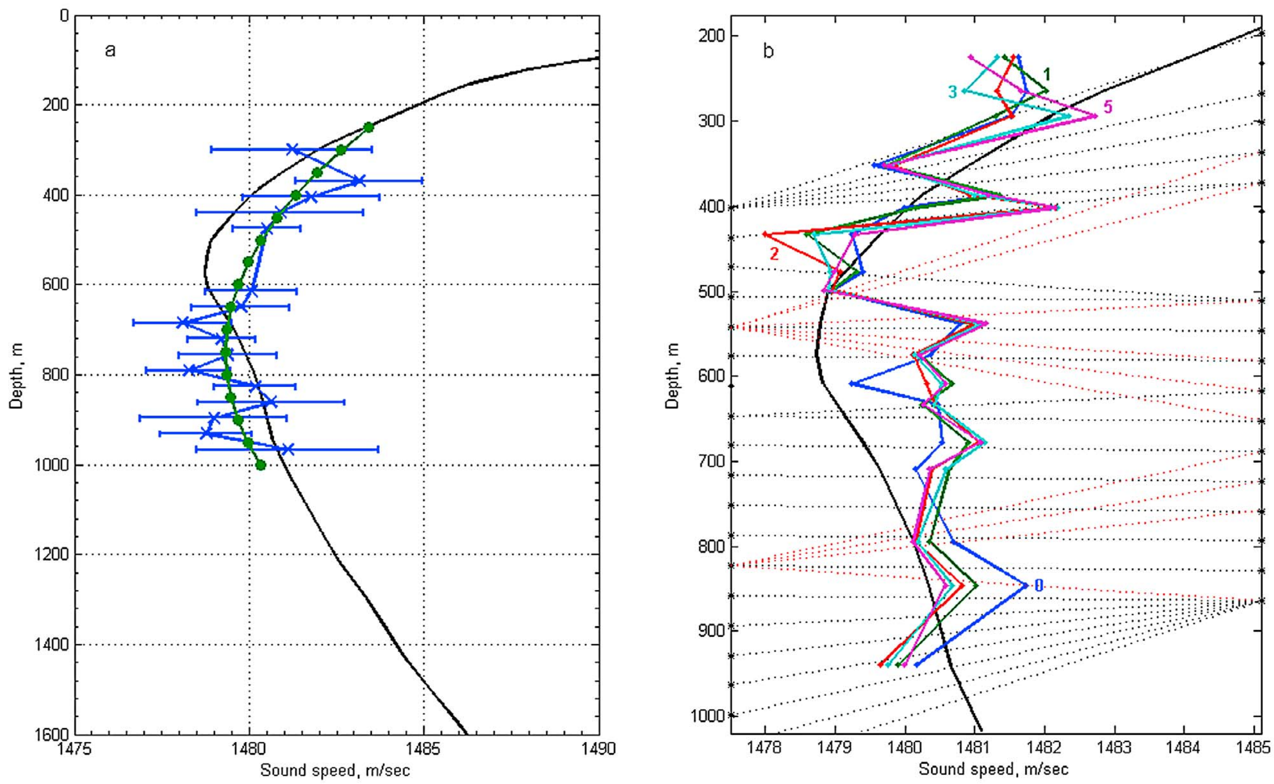


**Figure 4.** Inversion of passively measured acoustic travel times. Sound-speed profiles are retrieved using either a (a) simple, blind inversion or (b) full tomographic inversion of the travel times between hydrophones on VLAs 1 and 5. Annual average sound-speed profile [*Worcester and Spindel*, 2005] is shown by solid black lines. In Figure 4a, blue dots with error bars and green dots show results of inversion for individual hydrophone pairs and the best-fitting parabola, respectively. In Figure 4b, sound-speed inversions obtained using different number of ray paths per VLA 1 hydrophone are distinguished by color.

surement errors with each other and, below 700 m, with the annual average sound speed profile. The sound speed values obtained in this way should be treated as averaged over the time period required to accumulate the NCCF (few tens of hours) and over the horizontal distance between the VLAs involved (~3.5 km).

## 5. Conclusion

[14] Using the NPAL Billboard Array data, we have shown that cross-correlations of ambient noise measurements at spatially separated vertical line arrays of hydrophones in the ocean contain valuable information about the sound-speed field between the arrays. Noise anisotropy in the horizontal and vertical planes has a profound effect on the necessary data accumulation times and the amount of environmental information recoverable from the NCCF. A preponderance of uncontrolled localized noise sources makes the Billboard Array site particularly and, perhaps, uncharacteristically challenging for retrieval of oceanographic information from ambient noise. The suppression of contributions of localized noise sources to the ambient noise field proved necessary in order to use the NCCF for environmental characterization. Often, but not always, "kurtosis screening" of the data makes the noise field effectively more diffuse and leads to improved acoustic travel-time retrieval from the NCCF. We have demonstrated that acoustic daylight can be successfully used to measure sound-speed profiles with accuracy suitable for oceanographic applications. Further research is needed to determine the feasibility of ocean thermometry and tomography with acoustic daylight at longer ranges of tens and hundreds of kilometers.

[15] Our results strongly suggest that a dedicated passive acoustic system can be employed for cost-effective, long-term, depth-resolving observations of variations in the temperature field and heat content in the ocean.

[16] **Acknowledgments.** The noise data were obtained by the NPAL Group (J. A. Colosi, B. D. Cornuelle, B. D. Dushaw, M. A. Dzieciuch, B. M. Howe, J. A. Mercer, W. H. Munk, R. C. Spindel, and P. F. Worcester) and were made available for this study by P. F. Worcester. Helpful suggestions by A. G. Voronovich are gratefully acknowledged. This work was supported by the Office of Naval Research through grant N00014-08-1-0100.

## References

Baggeroer, A. B., E. K. Scheer, and the NPAL Group (2005), Statistics and vertical directionality of low-frequency ambient noise at the North Pacific Acoustic Laboratory site, *J. Acoust. Soc. Am.*, *117*, 1643–1665, doi:10.1121/1.1855035.

Brooks, L. A., and P. Gerstoft (2009), Green's function approximation from cross-correlations of 20–100 Hz noise during a tropical storm, *J. Acoust. Soc. Am.*, *125*, 723–734, doi:10.1121/1.3056563.

Fried, S. E., W. A. Kuperman, K. G. Sabra, and P. Roux (2008), Extracting the local Green's function on a horizontal array from ambient ocean noise, *J. Acoust. Soc. Am.*, *124*, EL183–EL188, doi:10.1121/1.2960937.

Godin, O. A. (2006), Recovering the acoustic Green's function from ambient noise cross-correlation in an inhomogeneous moving medium, *Phys. Rev. Lett.*, *97*, 054301, doi:10.1103/PhysRevLett.97.054301.
Godin, O. A. (2009a), Emergence of deterministic Green's functions from noise generated by finite random sources, *Phys. Rev. E*, *80*, 066605, doi:10.1103/PhysRevE.80.066605.
Godin, O. A. (2009b), Passive acoustic techniques for monitoring ocean dynamics, *Eos Trans. AGU*, *90*(22), Jt. Assem. Suppl., Abstract OS23C-04.
Godin, O. A. (2010), Cross-correlation function of acoustic fields generated by random high-frequency sources, *J. Acoust. Soc. Am.*, in press.
Goncharov, V. V., V. Y. Zaitsev, V. M. Kurtepov, A. G. Nechaev, and A. I. Khilko (1997), *Ocean Acoustic Tomography* (in Russian), chap. 2, Inst. of Appl. Phys., Nizhny Novgorod, Russia.
Gouédard, P., et al. (2008), Cross-correlation of random fields: Mathematical approach and applications, *Geophys. Prospect.*, *56*, 375–393, doi:10.1111/j.1365-2478.2007.00684.x.
Rickett, J., and J. Claerbout (1999), Acoustic daylight imaging via spectral factorization: Helioseismology and reservoir monitoring, *Leading Edge*, *18*, 957–960, doi:10.1190/1.1438420.
Roux, P., W. A. Kuperman, and the NPAL Group (2004), Extracting coherent wave fronts from acoustic ambient in the ocean, *J. Acoust. Soc. Am.*, *116*, 1995–2003, doi:10.1121/1.1797754.
Siderius, M., H. Song, P. Gerstoft, W. S. Hodgkiss, P. Hursky, and C. H. Harrison (2010), Adaptive passive fathometer processing, *J. Acoust. Soc. Am.*, *127*, 2193–2200, doi:10.1121/1.3303985.
Snieder, R. (2004), Extracting the Green's function from the correlation of coda waves: A derivation based on stationary phase, *Phys. Rev. E*, *69*, 046610, doi:10.1103/PhysRevE.69.046610.
Wapenaar, K., D. Draganov, and J. O. A. Robertsson (Eds.) (2008), S*eismic Interferometry: History and Present Status*, *Geophys. Reprint Ser.*, vol. 26, Soc. of Explor. Geophys., Tulsa, Okla.
Worcester, P. F., and R. C. Spindel (2005), North Pacific Acoustic Laboratory, *J. Acoust. Soc. Am.*, *117*, 1499–1510, doi:10.1121/1.1854780.

O. A. Godin and N. A. Zabotin, Cooperative Institute for Research in Environmental Sciences, University of Colorado at Boulder, 425 UCB, Boulder, CO 80309, USA. (oleg.godin@noaa.gov)
V. V. Goncharov, P. P. Shirshov Oceanology Institute, Russian Academy of Sciences, 36 Nakhimovski Ave., Moscow 117997, Russia.